MIT Open Access Articles

CONSTRAINTS ON THE UNIVERSAL C IV MASS DENSITY AT z ~ 6 FROM EARLY IR SPECTRA OBTAINED WITH THE MAGELLAN FIRE SPECTOGRAPH

Massachusetts Institute of Technology

CONSTRAINTS ON THE UNIVERSAL C IV MASS DENSITY AT $Z \sim 6$ FROM EARLY IR SPECTRA OBTAINED WITH THE MAGELLAN FIRE SPECTROGRAPH[1]

Robert A. Simcoe[2,8], Kathy L. Cooksey[2,9], Michael Matejek[2], Adam J. Burgasser[2,3,10], John Bochanski[2,4], Elizabeth Lovegrove[2,5], Rebecca A. Bernstein[5], Judith L. Pipher[6], William J. Forrest[6], Craig McMurtry[6], Xiaohui Fan[7], and John O'Meara[11]

Draft version April 22, 2011

ABSTRACT

We present a new determination of the intergalactic C IV mass density at $4.3 < z < 6.3$. Our constraints are derived from high signal-to-noise spectra of seven quasars at $z > 5.8$ obtained with the newly commissioned FIRE spectrograph on the Magellan Baade telescope, coupled with six observations of northern objects taken from the literature. We confirm the presence of a downturn in the C IV abundance at $\langle z \rangle = 5.66$ by a factor of 4.1 relative to its value at $\langle z \rangle = 4.96$, as measured in the same sightlines. In the FIRE sample, a strong system previously reported in the literature as C IV at $z = 5.82$ is re-identified as Mg II at $z = 2.78$, leading to a substantial downward revision in $\Omega_{\rm C\,IV}$ for these prior studies. Additionally we confirm the presence of at least two systems with low-ionization C II, Si II, and O I absorption but relatively weak signal from C IV. The latter systems systems may be of interest if the downward trend in $\Omega_{\rm C\,IV}$ at high redshift is driven in part by ionization effects.

1. INTRODUCTION

In March 2010, our group commissioned the Folded-Port Infrared Echellette (FIRE), a new IR echelle spectrograph for the 6.5 meter Magellan Baade Telescope. FIRE delivers $R = 6000$ spectra with uninterrupted coverage from 0.82 to 2.5 μm for a 0.6″ slit (Simcoe et al. 2010, 2011). One of the major science drivers for its construction was exploration of the high-redshift intergalactic medium (IGM) via absorption line spectroscopy. Here, we report initial results on the search for high-redshift C IV based on commissioning observations taken during the first year of FIRE's operation.

The existence of heavy elements in the intergalactic medium (IGM) has been known since the earliest detections of C IV associated with $z \sim 3$ Ly-α forest absorbers in high resolution optical spectra (Cowie et al. 1995; Songaila & Cowie 1996; Cowie & Songaila 1998). Soon after this discovery, intergalactic C IV lines were detected even in the spectra of quasars with $z > 4$, establishing a lower limit on the amount of metal production that must have occurred in the early universe (Songaila 2001). A surprising result of these studies was the relatively constant comoving number density of C IV atoms over a wide range in redshift, where this density is smoothed over very large scales. More recent UV observations at low redshift (Cooksey et al. 2010;

Danforth & Shull 2008) point toward a slow rise in the C IV density—expressed as $\Omega_{\rm C\,IV}$, the C IV contribution to closure—increasing by a factor of three to four between $z \sim 2$ and the present day.

The discovery of luminous quasar populations at $z > 6$ (Fan et al. 2006; Willott et al. 2010; Mortlock et al. 2009) enables studies of the C IV density at higher redshift, but above $z \sim 5.5$ observations become challenging as the C IV transition moves into the Y and J bands. For this reason, the earliest pilot studies in this region focused on very small (i.e. $N = 2$) samples of quasar sightlines. These pilot studies yielded similar values of $\Omega_{\rm C\,IV}$ as at lower z, but with few actual line detections they were strongly affected by small number statistics (Simcoe 2006; Ryan-Weber et al. 2006; Becker et al. 2009). More recently Ryan-Weber et al. (2009) compiled a larger set of IR observations for 9 QSOS, with VLT/ISAAC and Keck/NIRSPEC. Their dataset contains several sightlines with no C IV detections, which points to a decrease in $\Omega_{\rm C\,IV}$ at $z > 5.5$.

During FIRE's first year of operation we have obtained spectra of eleven $z > 5.5$ quasars, of which eight have suitable signal-to-noise ratio (SNR) for IGM abundance measurements. This paper presents a first analysis of seven of these spectra, focusing on the search for C IV doublets in particular. We combine our results with data from the literature to derive a new value for $\Omega_{\rm C\,IV}$ based on 13 unique sightlines. Where relevant throughout the remainder of the paper, we adopt a flat cosmology with $\Omega_M = 0.3$, $\Omega_\Lambda = 0.7$, and $H_0 = 71$ km s^{-1} Mpc.

2. OBSERVATIONS AND DATA REDUCTIONS

During the period from 31 March 2010 to 3 April 2011, we obtained FIRE spectra of 11 QSOs with $z_{em} > 5.5$, of which eight had high enough SNR to study IGM absorption. Table 1 lists details of the observations for the seven high-redshift targets included in the present analysis. All spectra were obtained with a 0.6″ slit, in seeing conditions ranging from 0.35–0.9″, for a measured resolution of $R = 6000$, or 50 km s^{-1}. Individual integration

[1] This paper includes data gathered with the 6.5 meter Magellan Telescopes located at Las Campanas Observatory, Chile.
[2] MIT-Kavli Center for Astrophysics and Space Research
[3] Center for Astrophysics and Space Science, University of California, San Diego, La Jolla, CA, 92093, USA
[4] Pennsylvania State University, Department of Astronomy and Astrophysics, 525 Davey Lab, University Park, PA 16802, USA
[5] University of California, Santa Cruz
[6] University of Rochester
[7] University of Arizona
[8] Sloan Foundation Research Fellow
[9] NSF Fellow
[10] Hellman Fellow
[11] St. Michael's College

times are listed in the table, with typical values of 4-5 hours. Full integrations were broken up into 15- to 20-minute intervals between which the object was moved on the slit.

We reduced the data using a custom-developed IDL pipeline, evolved from the MASE suite used for optical echelle reduction (Bochanski et al. 2009). There were several important modifications implemented for IR work. The most important of these was for wavelength calibration, which is principally solved using the terrestrial OH lines imprinted upon science spectra. Unlike most IR spectral packages which perform pairwise subtraction of A/B slit positions for sky subtraction, the FIRE pipeline instead calculates a direct B-spline model of the sky for each exposure using the techniques of Kelson (2003). This yields Poisson-limited residuals in the sky-subtracted frame, for a theoretical improvement of $\sqrt{2}$ in SNR relative to pairwise subtraction. This pipeline is being released to the community as part of the instrument package; a full description of its functionality and the efficacy of the sky subtraction will be provided in a separate forthcoming paper.

During observations, we obtained contemporaneous spectra of A0V stars for correction of telluric absorption features using the method of Vacca et al. (2003). We used the `xtellcor` procedure released with the `spextool` pipeline (Cushing et al. 2004) to perform telluric correction and relative flux calibration, finally combining the corrected echelle orders from all exposures into a single, 1D spectrum for analysis.

For each sample target, we obtained additional far-optical spectra using the Magellan Echellette spectrometer (MagE, Marshall et al. 2008), for the purpose of augmenting SNR in the region blueward of 9000Å. These spectra had typical integration times of ~ 1 hour, and $R = 5600$, a close match to FIRE. The data were processed in similar fashion as described above. Rather than performing detailed telluric corrections to the MagE data, we instead masked out regions susceptible to telluric contamination when combining with the FIRE spectra, only including the MagE contribution in telluric-free areas. The MagE spectra were smoothed to match the resolution of FIRE and the spectra from the two instruments were combined with inverse variance weighting, to create a single composite for analysis.

3. ANALYSIS

3.1. *Line Identification*

Before searching the data for C IV doublets, we fit a smooth continuum estimate to each quasar spectrum using a slowly-varying cubic spline. Figure 1 displays the C IV region for each of the continuum-normalized spectra. These regions were then searched both by hand and also using automated software to identify C IV doublets.

The automated search algorithm followed a two step process. First, the inverse spectrum ($1 - f/f_0$, where f is the flux and f_0 the continuum) was smoothed with a Gaussian kernel having full-width at half-maximum (FWHM) of one spectral resolution element—i.e. 50 km s^{-1} or 4 pixels. A peak finding procedure was run on the convolved spectrum to identify all deviations of $\geq 2.5\sigma$, which after convolution is equivalent to the SNR per resolution element.

TABLE 1
FIRE OBSERVATIONS

Object	z	J^1	Exptime (s)	Δz	ΔX
SDSS 0818+1722	6.00	18.5	9,000	4.50-6.00	5.61
SDSS 0836+0054	5.82	17.9	10,187	4.35-5.79	4.52
SDSS 1030+0524	6.28	18.9	14,400	4.75-6.29	6.82
SDSS 1306+0356	6.01	18.8	15,682	4.52-5.97	6.46
ULAS 1319+0905	6.13	18.9	19,275	4.62-6.08	6.56
SDSS 1411+1217	5.93	18.9	15,300	4.55-5.93	5.28
CFHQS 1509–1749	6.12	18.9	17,100	4.60-6.11	6.03

[1] Vega magnitudes

This list of single-line identifications was then parsed to identify pairs at the appropriate velocity spacing for C IV doublets. We further required that the ratio of the absorption amplitudes between the 1548Å and 1551Å lines be consistent with the ratio in oscillator strengths, i.e. between 2.0 (for an unsaturated doublet) and 1.05 (completely saturated). Each candidate whose doublet ratio fell within $\pm 1\sigma$ of this range was inspected visually to reject obvious anomalies, for example from poor sky subtraction near OH sky lines. We also verified that candidate C IV pairs were not Si II/O I doublets at higher redshift, by inspecting the corresponding C IV and Mg II wavelengths, as well as Si II λ1526Å for each system that could be mis-identified in this way.

3.2. *Completeness Estimates*

At $z \lesssim 4$, the C IV column density distribution has a power law form extending at least to $N_{\rm C\ IV} = 10^{12.5-13.0}$ and possibly lower, as measured from high SNR, high resolution optical spectra (Ellison et al. 2000; Songaila 2001, 2005). Our high redshift sample is incomplete at these lower column densities, because of our $\sim 10\times$ lower resolution (e.g. compared to HIRES) and $\sim 5\times$ lower SNR when compared with the best optical QSO spectra in the literature.

To quantify this incompleteness, we ran a simple set of Monte Carlo tests where a simulated C IV signal was injected into our actual QSO spectra. Our line finding algorithm was then run to determine the recovery fraction as a function of redshift, column density, and line width b.

The intrinsic properties of $z \sim 6$ C IV lines are not yet well-characterized because the largest existing surveys are likely limited by instrumental resolution rather than intrinsic line widths[12]. At lower redshift, typical b parameters take values in the range $b \sim 8 - 20$ km s^{-1}, with a slight preference for larger b at higher column densities. For the completeness tests, we took a forward-modeling approach by drawing b parameters at random from a distribution matched to HIRES C IV fits at $z \sim 2 - 3$ (Rauch et al. 1996). This distribution is Gaussian in shape, and centered at 10 km s^{-1} for $N_{\rm C\ IV} = 10^{13}$. It has a cutoff below 5 km s^{-1} and a steady rise in the mean b to 15 km s^{-1} at $N_{\rm C\ IV} = 10^{14}$ but again cuts off above $b \sim 25$ km s^{-1}.

Over a grid of column density, we drew redshifts at random, with a distribution matched to the pathlength-

---

[12] The NIRSPEC spectra of Becker et al. (2009) with resolution 23 km s^{-1} may sample the high end tail of the b distribution at lower SNR, but the present study and others in the literature are a factor of ~ 2 lower resolution.
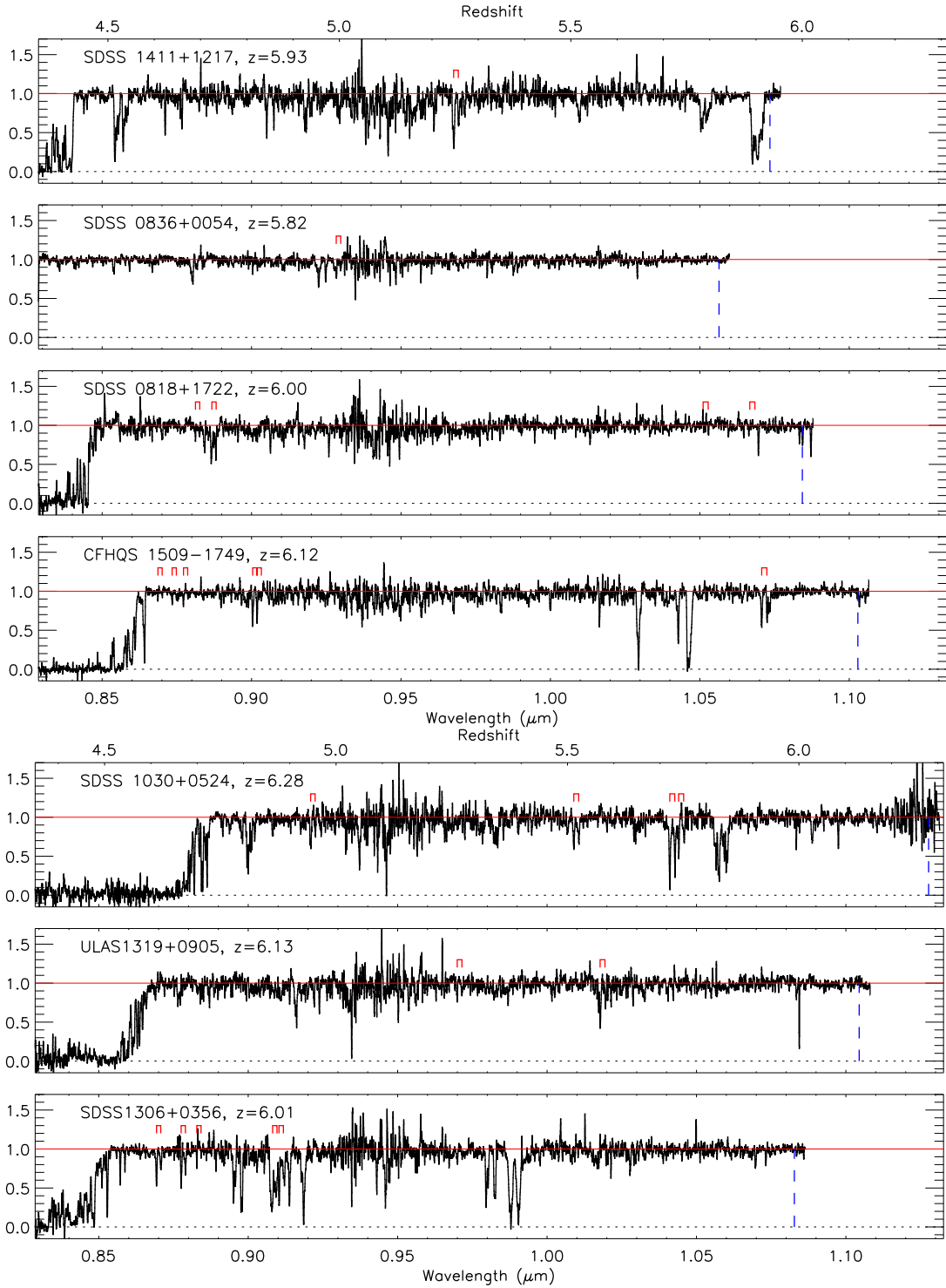
FIG. 1.— Normalized spectra of the seven sample objects, ranging from the minimum search redshift ($z = 4.35$ in SDSS0836+0054) to the maximum $z = 6.3$ (in SDSS1030+0524). The locations of C IV doublet in Table 2 are shown with red marks, and the C IV wavelength at the QSO emission redshift is shown as a vertical dashed line. The weaker C IV systems that are difficult to see in this plot are better displayed in Figure 3.
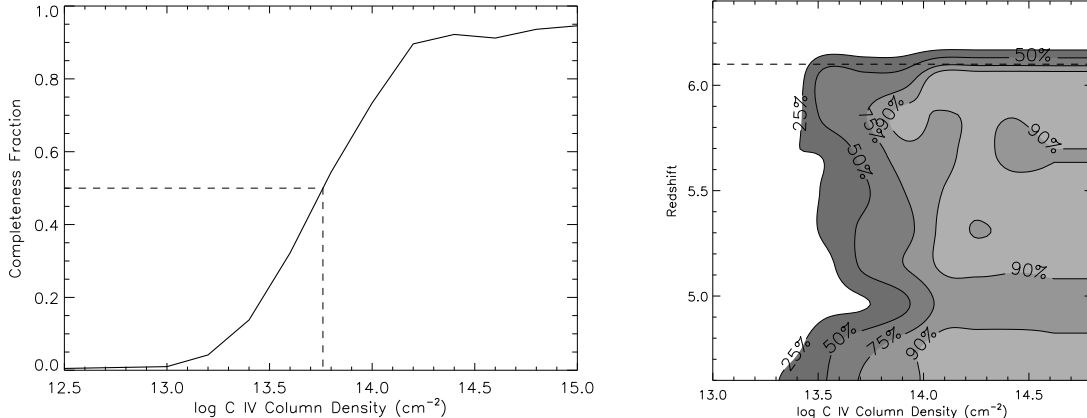
Fig. 2.— *Left:* The combined C IV sample completeness averaged over the full path of the survey. Dotted lines show the 50% completeness level, which occurs around $N_{\rm C\,IV} = 10^{13.75}\,{\rm cm}^{-2}$. *Right:* The distribution of completeness with C IV column density and redshift. Some redshift ranges—particularly near $z = 5.0$—have lower completeness because of higher noise levels in the data. This dependence is taken into account when correcting each detected line up for incompleteness when determining $\Omega_{\rm C\,IV}$.

weighted redshift distribution of the survey sightlines. We then calculated Voigt profiles directly for each artificial line, convolved these with the instrumental response function, and inserted them to the survey spectra, with one artificial system, per spectrum, per trial.

We then re-ran the line search algorithm described above on each trial spectrum and examined the output to see if the line was recovered. Each successful recovery was inspected by eye to ensure that our completeness was not being over-estimated due to chance correlations in noise being picked up as "detections" for intrinsically weak lines. This procedure was repeated 5000 times, with 500 trials at each point in a grid of $N_{\rm C\,IV}$ between 10^{13} and 10^{15} cm^{-2}.

Figure 2 shows the total completeness distribution of the survey; the left panel includes all z while the right panel shows the completeness map by both redshift and $N_{\rm C\,IV}$. Broadly speaking, we recover most lines ($> 80\%$) above $N_{\rm C\,IV} = 10^{14}$ and relatively few ($< 10\%$) below $N_{\rm C\,IV} = 10^{13.2}$, with the 50% level occurring near $10^{13.7}$. Thus our survey sits between the parameter space explored by Becker et al. (2009), who are complete to lower $N_{\rm C\,IV}$ over a significantly smaller pathlength, and Ryan-Weber et al. (2009) who have a comparable pathlength but slightly lower completeness.

From the right panel of Figure 2 it is also apparent that the completeness varies with search redshift, with our areas of highest sensitivity occurring at $z < 4.8$ and $z > 5.2$. The high completeness at $z > 5.7$ reflects the rising sensitivity of FIRE toward these wavelengths, while at $z < 4.8$ the MagE spectra contribute significantly to the SNR. The relatively low completeness at $z \sim 5$ results from decreased flux and/or imperfect correction in the vicinity of telluric absorption bands, which can be seen as increased noise around $\lambda = 0.94\mu$m in Figure 1.

In statistical calculations below, we correct for incompleteness by scaling each detected line by the inverse of its estimated completeness fraction. It is worth noting that the C IV lines reported in the literature to date nearly all have $N_{\rm C\,IV} > 10^{14}$ cm^{-2}; we should detect the large majority of these over our entire survey volume, so the correction to $\Omega_{\rm C\,IV}$ from this source of incompleteness is only $\sim 25\%$ or 0.1 dex - smaller than the Poisson

errors from the limited number of systems in the sample. At smaller column density the correction is more severe, but these systems make a smaller fractional contribution to the total value of $\Omega_{\rm C\,IV}$.

4. C IV SAMPLE AND MEASUREMENTS

Using the criteria described above, we identified 19 unique C IV systems ranging in redshift from $z = 4.61$ to $z = 5.92$ in the six survey sightlines. Properties of the individual systems are listed in Table 2, and plots of the individual absorbers are shown in Figure 3. We excluded regions within 3000 km s^{-1} of the QSO emission redshift from the search; however, no lines were excluded by this criterion, except for the one BAL absorber in SDSS1411. The Table contains two additional systems in SDSS0818+1722 at $z = 5.789$ and $z = 5.876$; these systems were not flagged as C IV in our data but have been reported previously in the literature and are discussed in Section 4.8.1.

We characterized the absorption strength for each system using a variety of different methods and to test the robustness of our column density determinations. At a resolution of 50 km s^{-1} we almost certainly fail to resolve the detailed velocity structure seen in C IV systems at lower redshift, and we must also be attuned to the possibility of unresolved saturated components.

For each system, we list the rest-frame equivalent width (W_r) of both transitions of the C IV doublet, determined by direct summation of the continuum-normalized spectral pixels. The sums were performed over a region 50 km s^{-1} above and below where the normalized profile returns to unity. We then list a C IV column density as determined using the "apparent optical depth" method of Savage & Sembach (1991), and finally the column density and b parameter estimates from direct Voigt profile fitting using the `vpfit` package.

Inspection of the Voigt profile Doppler parameters in Table 2 shows a high average b, similar to what was described in Ryan-Weber et al. (2009). This width is more likely to represent the full velocity spread of a suite of narrow components, rather than a large, single component. However, in such cases the *total* column density of the system is represented surprisingly well in a profile fit, since the ratio of the absorption depths reflects the
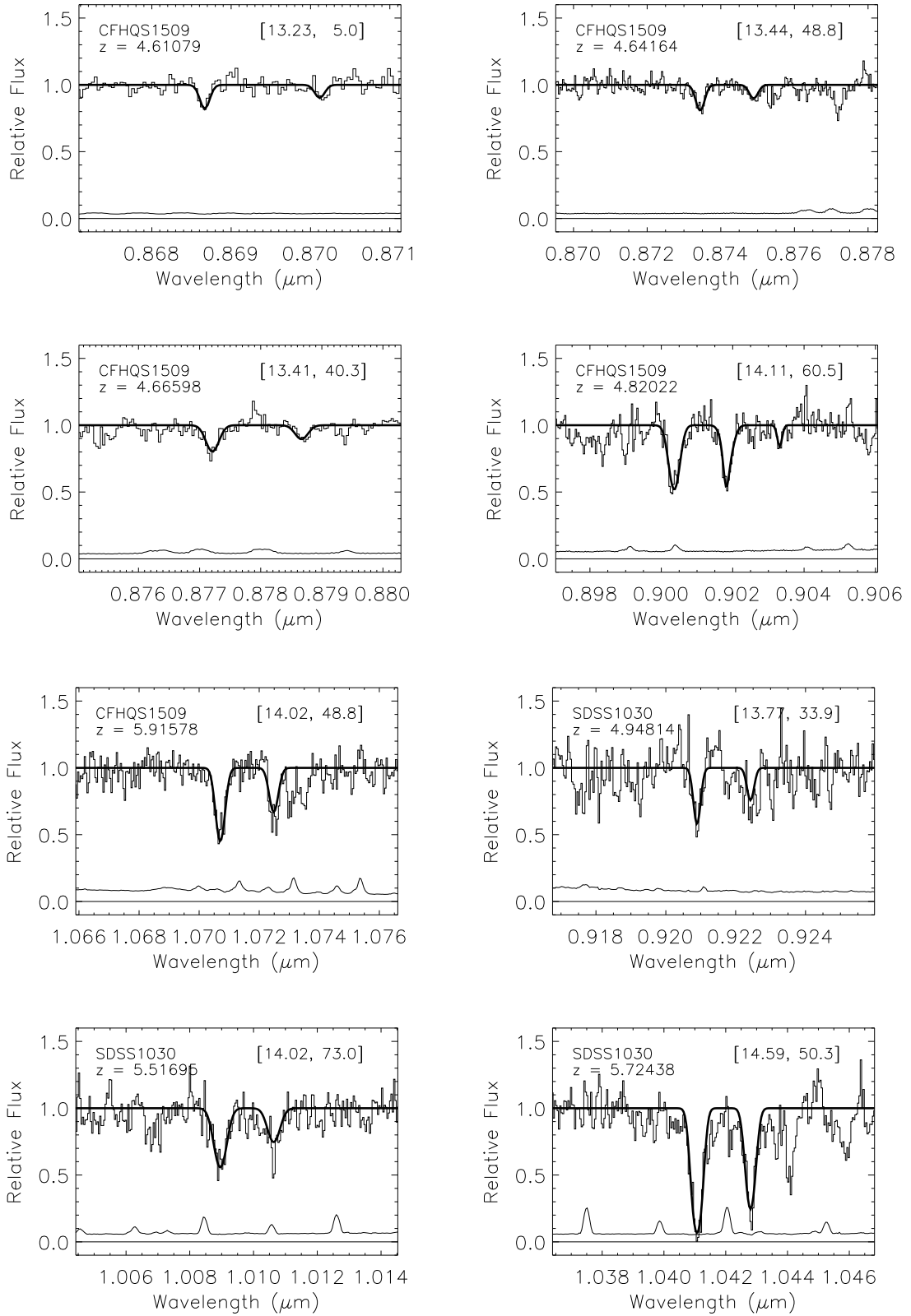
FIG. 3.— Plots of individual C IV systems listed in Table 2, in units of continuum normalized flux. The 1σ error array is shown at bottom, and a best-fit Voigt profile is shown with a solid smooth line. The total $\log(N_{\mathrm{C\,IV}})$ and b is shown for each system in square brackets.

degree of saturation (i.e. the column density for a single component) and the b parameter then scales with the number of individual sub-clumps in the system.

4.1. *SDSS0818+1722, $z_{em} = 6.00$*

We detect two discrete C IV systems toward this QSO, which had the shortest total integration of our sample. One of our detections, at $z = 4.7266$, is very robust and appears to contain at least two subcomponents. There is some hint of further substructure in the profile but the SNR of our data did not warrant a more aggressive fit. The second system we detect is at $z = 4.6919$ and is very weak at $N_{\rm C\,IV} = 10^{13.2-13.4}$.

This sightline has also been observed with ISAAC (Ryan-Weber et al. 2009), NIRSPEC (Becker et al. 2009) and XShooter (D'Odorico et al. 2011). From these studies the system at $z = 4.7266$ is confirmed but the system at 4.6919 is not. In addition, Ryan-Weber et al. (2009) and D'Odorico et al. (2011) report tentative C IV detections at $z = 5.7892$ and $z = 5.8769$, respectively. These systems are discussed further in Section 4.8.1. The $z = 5.7892$ system appears to suffer from sky subtraction systematics in the FIRE spectrum, and may be consistent with C IV absorption. The $z = 5.8769$ is detected in C IV 1548Å, but the 1550Å component of the doublet narrowly misses our 2.5σ threshold. However we confirm the clear presence of low-ionization gas associated with both these systems. Since they are not formally detected in the FIRE spectrum, we do not include these systems in our statistical calculations, although they would represent only a 0.08 dex perturbation on the final mass density calculation. D'Odorico et al. (2011) report a very large number of additional systems (13, at $z = 4.498, 4.508, 4.523, 4.552, 4.577, 4.620, 4.732, 4.877, 4.942, 5.076, 5.308, 5.322,$ and 5.344) which we do not detect in our 9000s spectrum. The systems at $z \lesssim 5$ are detected in neither our MagE or FIRE spectra, and so must be quite weak. The higher redshift examples may only be revealed at the higher SNR revealed by D'Odorico's 24,000s spectrum.

4.2. *CFHQS1509–1749*

We detect 5 unique systems in our FIRE spectrum of CFHQS1509–1749. Four of these are quite weak at $z < 5$, while one at $z = 4.820$ is significant. The systems at $z = 4.6108, 4.6416,$ and 4.6659 were reported by D'Odorico et al. (2011), but the system at $z = 4.820$ was not. A second weak component was required to obtain a good fit on the $z = 4.8202$ system to avoid reversing the doublet ratio.

We detect an additional system not previously reported at $z = 5.9158$; this is the highest redshift C IV system in our sample, and to our knowledge the highest redshift absorption system currently known. The C IV system listed at $z = 4.820$ is closely matched in wavelength to the expected location of the O I/Si II pair, but this alternate identification is ruled out by a lack of Si II $\lambda1526$Å.

4.3. *SDSS1030+0524*

We detect three distinct systems in SDSS1030+0524, and retract from this sightline a fourth system that has been discussed in the literature. The first system is at $z = 5.7244$ and was a strong detection reported by Ryan-Weber et al. (2006) and a marginal detection in Simcoe (2006). In addition, we find new systems at $z = 4.9481$ and $z = 5.5169$. The $z = 4.9481$ system is confirmed by the presence of Si II 1526Å, Al II 1670Å, and the Mg II doublet, while the $z = 5.5169$ system is confirmed by Si II 1526Å, Fe II (multiple lines), and Al II 1670Å(Mg II falls between the H and K bands). We detect an additional C IV doublet at $z = 5.744$, in the vicinity of the known system at $z = 5.72$. However the strong absorption system at $1.057\mu m$—previously identified as C IV—is shown in the FIRE spectrum to be a remarkable low redshift interloping Mg II system (discussed further in Section 4.8.2)

4.4. *SDSS0836+0054*

This bright, lower redshift QSO has been observed by the groups noted above, with no C IV detections. Despite excellent SNR, we also detect no C IV absorption at $z > 5$, although we do detect a new system at $z = 4.996$, with possible Si IV seen at the 2σ level. At $z > 5$, this sightline is roughly 0.2 dex more sensitive than the survey average: its 50% completeness falls at $\log(N_{\rm C\,IV}) = 13.55$, and is 80% complete at $\log(N_{\rm C\,IV}) = 13.8$.

4.5. *SDSS1411+1217*

This spectrum had among the lowest SNR of our sample given its ratio of emission line to continuum flux. However we detected one very strong C IV system at $z = 5.2498$ which shows evidence of velocity structure in its profile. This system is also seen in Mg II and Si IV; C II and Si II are not detected but also not strongly ruled out by the data. Fe II falls in a high SNR region of the spectrum but was not detected.
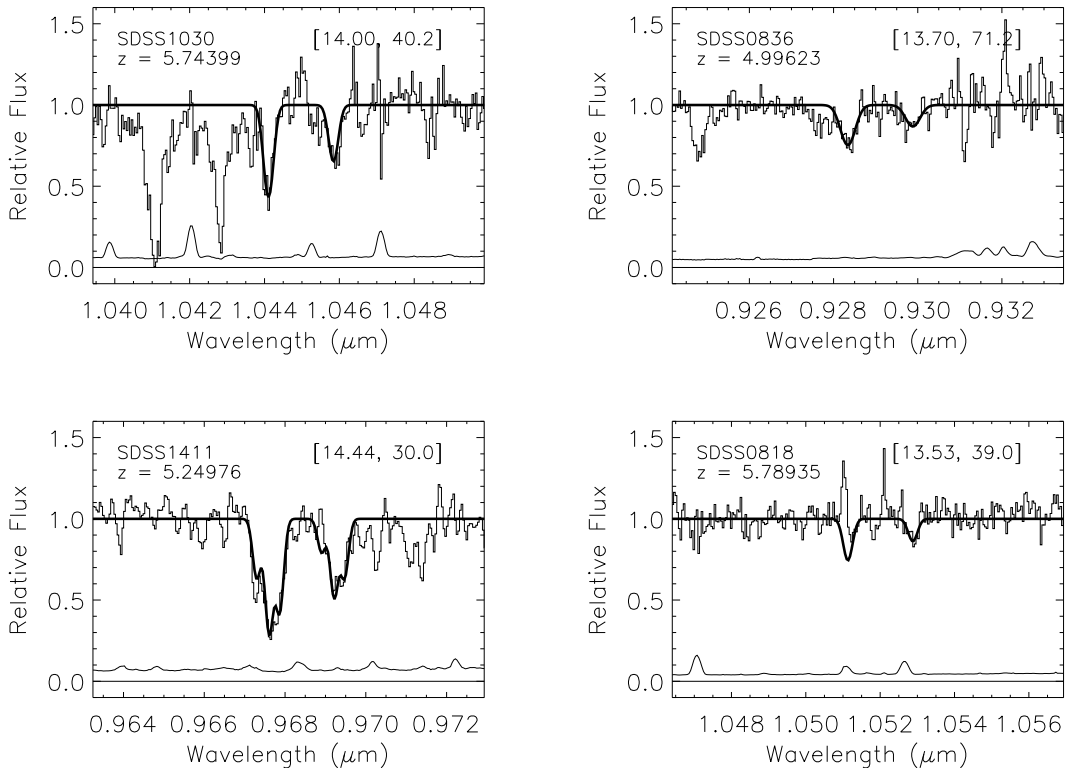
There is a high redshift absorber that appears to be C IV near $z = 5.786$, but this line has extremely extended absorption as would be characteristic of a BAL at the redshift of the background QSO, so we do not include it in the IGM sample.

4.6. *ULAS1319+0950*

This sightline has not previously been observed for C IV absorption. We detect a significant C IV system at $z = 5.573$, which is accompanied by strong Si IV , possible C II , and Fe II . A second, very marginal detection is seen at $z = 5.2646$ with no other transitions. More sensitive data are needed to confirm the identification of this system.

4.7. *SDSS1306+0305*

Three C IV systems are detected in the lower-redshift region of this spectrum, including a very strong complex at $z = 4.870$ that also displays Si II, Fe II, Al II, Mg II, and possible Mg I . This system was also seen in the optical spectra of Becker et al. (2001). Significant systems are also detected at $z = 4.613$ and 4.686; a weak system is possibly present at $z = 4.702$ but is only detected at 2σ significance and so is not included in the sample. Similar to previous studies of this sightline, we find no statistically significant C IV absorption at $z > 5$. The two strong absorption lines at 9900Å are from an interloping Mg II system at $z = 2.53$.

FIG. 3.— *Continued*

4.8. *Special Cases*

4.8.1. *The z = 5.7899 absorber in SDSS0818*

Ryan-Weber et al. (2009) reported a possible C IV system in SDSS0818+1722 at $z = 5.7899$; this system was neither flagged in our visual inspection of the FIRE data nor found by our automated line search. However, as also reported by D'Odorico et al. (2011) and Becker et al. (2011), we do find evidence of low ionization absorption offset from the reported C IV redshift by ~ 75 km s^{-1}. A plot of several absorption species is shown in Figure 4, along with a shaded band showing the $\pm 1\sigma$ contours about the continuum.

Inspection of the error contour shows that both members of the C IV doublet are in regions of higher noise; this is because they are both blended with bright telluric OH emission lines at this redshift. There is weak evidence for absorption at the 1550Å component, but the 1548Å component appears to suffer from systematic sky subtraction effects. The data for this object were obtained on a single night (March 5, 2010) when the heliocentric velocity amplitude was 28 km s^{-1}, i.e. nearly radial towards SDSS0818. A revisit of this object with seasonal offset of $\sim 1/2$ year would effectively shift the telluric lines by one resolution element, providing an improved view of the absorber.
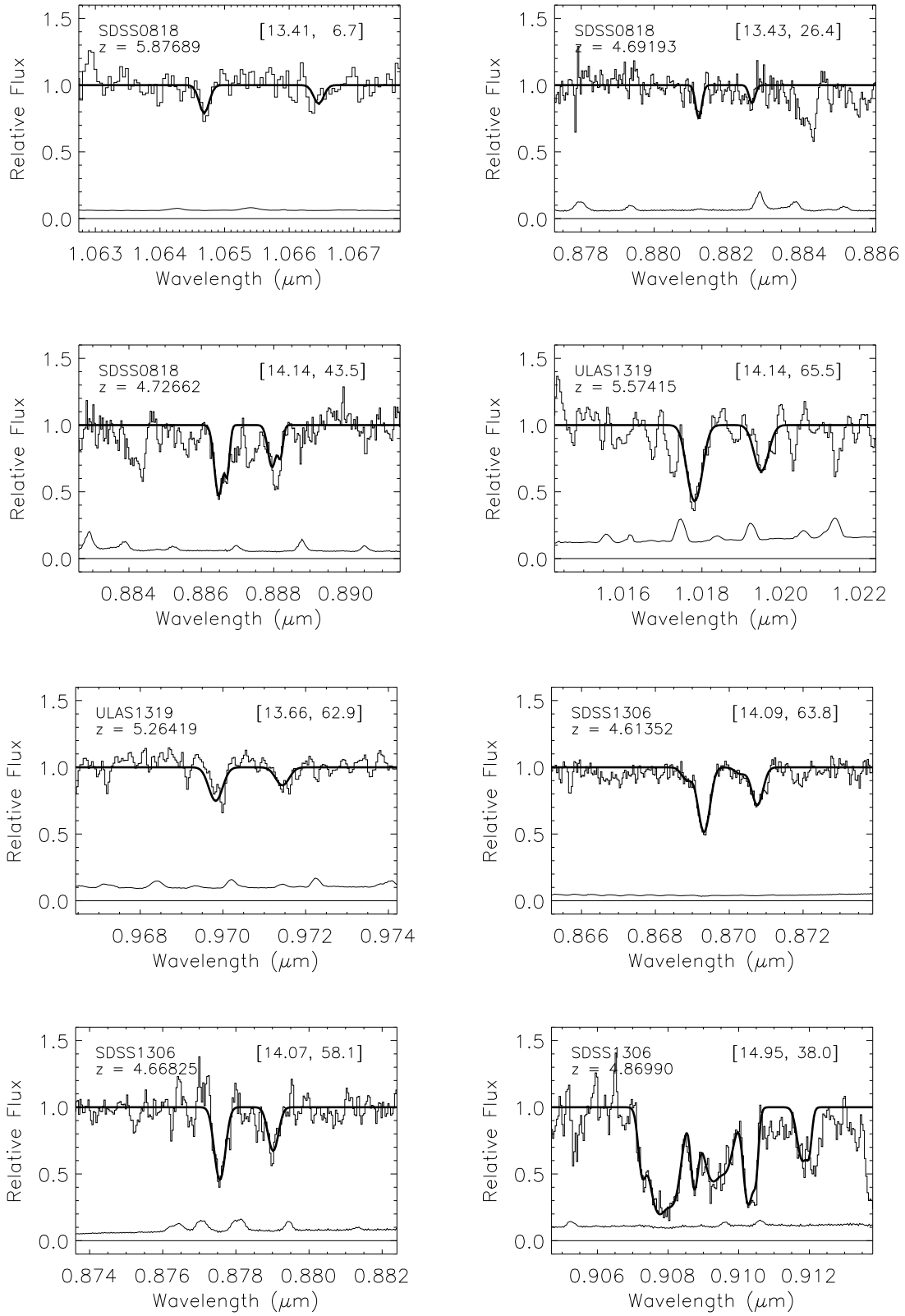
Using the 1550Å line alone, we fit a Voigt profile model to check for consistency in column density with the value reported by Ryan-Weber et al. (2009); the result is shown in the top panel of Figure 4. Based on this component, we verified that a $\log(N_{\rm C\ IV}) \approx 13.5$ C IV line represents our data quite well. Our fits con-

verged to lower values of the b parameter, though these may be unphysical since the values are well below one resolution element for FIRE. While the velocity width is uncertain, the total C IV column is roughly constant for any choice of $b < 39$ km s^{-1} (the value measured by Ryan-Weber et al. 2009).

This absorption system is intriguingly different from typical absorption line systems at lower redshift, where the neutral phase traced by O I, Fe II, Si II, and C II is usually accompanied by strong absorption from high-ionization species. In fact the presence of O I absorption suggests this system may be a damped Ly-α absorber or Super-Lyman-Limit system whose normal highly ionized gas phase is substantially suppressed.

4.8.2. *Re-identifying a reported high-z C IV system as Mg II*

Another finding with implications for the existing literature is our improved spectrum of SDSS 1030+0524, where a strong C IV system at $z = 5.8288$ was reported by both Simcoe (2006) and Ryan-Weber et al. (2009). This system was a marginal detection in the ISAAC spectrum, and Simcoe (2006) noted the presence of an unidentified, blended line in his GNIRS spectrum. In the FIRE spectrum, we clearly identify this absorber as a Mg II system at $z = 2.780$, based on the detailed match of the Mg II 2796 and 2803Å velocity profiles and the weak but detectable presence of Fe II absorption at coincident redshift. Figure 5 shows a stacked velocity plot of three transitions from the system along with a Voigt profile model fit for Mg II.
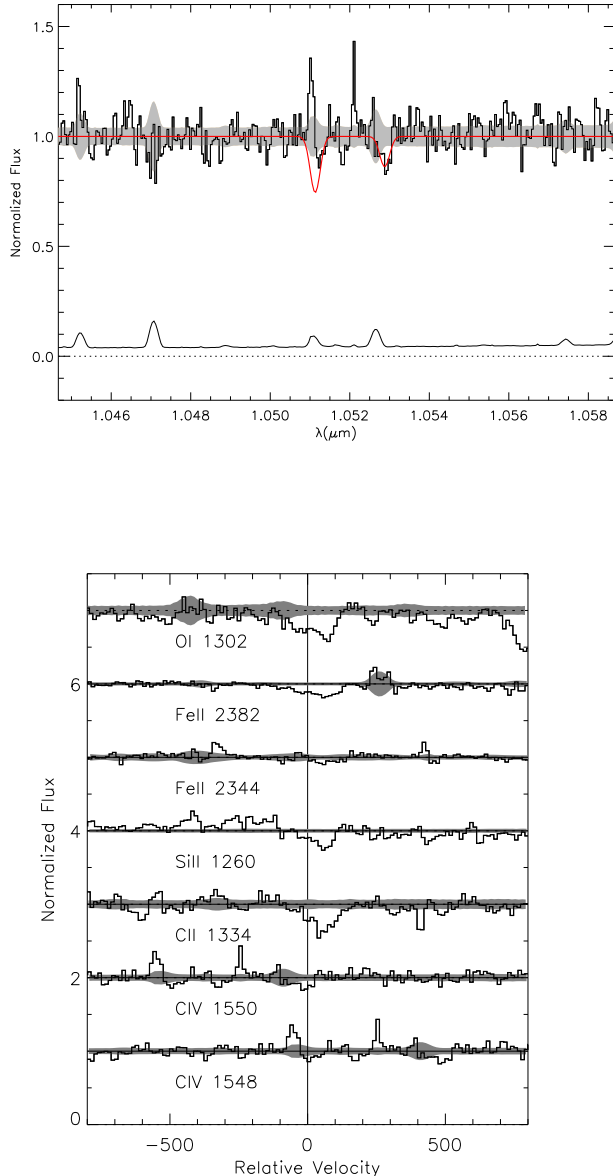
Fig. 3.— *Continued*

FIG. 4.— *Top:* FIRE spectrum showing the C IV region of SDSS0818+1722 at $z = 5.78990$, where both Ryan-Weber et al. (2009) and D'Odorico et al. (2011) report tentative detection of a weak C IV system. Gray region shows the $\pm 1\sigma$ error contours, while the solid black line shows a best-fit Voigt profile model to the 1550 Å component alone, which does *not* provide a good match to the 1548Å line. There is evidence of systematic error in the sky subtraction on the blue wing of the profile (the positive spike). *Bottom:* Confirmation of detected absorption in low ionization species at this redshift, including O I, Fe II, Si II, and C II.

We detect individual Mg II components[13] spanning a remarkable range of ± 400 km s^{-1}, and a total equivalent width in excess of 3Å. This places the system in the strongest 5% of absorbers with $W_r > 1$Å found in the SDSS (> 7000 systems at $0.35 < z < 2.3$ in the Sloan

---

[13] The term components here refers to distinct absorption features in the FIRE spectrum; at a resolution of $\Delta v = 50$ km s^{-1} it is very likely that each spectral resolution element contains several blended and/or saturated intrinsic components

DR3, Prochter et al. 2006). It also has a velocity width larger than any of the 22 Mg II systems studied at high resolution in Prochter et al. (2006).

The equivalent width for the $z = 2.78$ absorber qualifies it as a strong candidate Damped Lyman alpha system (Rao & Turnshek 2000), although the Ly-α line itself is inaccessible in the saturated forest. No coincident Mg I absorption is seen, so it is uncertain whether there is truly neutral gas present. This leaves the physical picture for this system uncertain. It may represent the chance interception of an unusually violent galactic outflow (Bond et al. 2001). Alternatively if a gravitational interpretation is invoked to explain the velocity spread, the associated potential must be somewhat large, up to galaxy group scales, unless the system is undergoing a merger or is otherwise out of dynamical equilibrium. If a large galaxy or small cluster potential is present at small enough impact parameter to be seen in Mg II absorption (generally $\lesssim 100h^{-1}$ physical kpc from galaxies, Chen et al. 2010), it is possible that this mass could act as a gravitational lens for SDSS1030, explaining in part its large apparent luminosity. A full analysis of this possibility is beyond the scope of the present paper.

4.9. *Effects on past determinations of* $\Omega_{C\ IV}$

The two systems discussed in sections 4.8.1 and 4.8.2 constitute 44% of the total C IV column density (and hence 44% of $\Omega_{C\ IV}$) reported in the Ryan-Weber et al. (2009) survey. The larger of these systems—containing 38% of the total C IV—is definitively removed from the sample, requiring a downward revision of $\Omega_{C\ IV}$ by a factor of 1.6. The smaller system is tentatively confirmed at the column density reported in Ryan-Weber et al. (2009), though this represents only a 6% fluctuation in $\Omega_{C\ IV}$.

Similar corrections must be applied for the results of Simcoe (2006) and Becker et al. (2009), which on account of their smaller sample sizes include a larger fractional contribution from the system in SDSS1030+0524. In the case of Simcoe (2006), the fractional contribution is a full 56%, leading to a $\sim 2\times$ downward revision in the derived $\Omega_{C\ IV}$. Becker et al detect *no* C IV systems explicitly in their NIRSPEC survey, but use the detections of Simcoe (2006) and Ryan-Weber et al. (2009) to set a lower bound on $\Omega_{C\ IV}$; this lower bound should be revised downward by a factor of ~ 2.

5. THE UNIVERSAL MASS DENSITY OF C IV

Using the C IV identifications listed in Table 2, we constructed an estimate of $\Omega_{C\ IV}$ using the customary form:

$$\Omega_{C\ IV} = \frac{1}{\rho_c} m_{C\ IV} \frac{\sum w_i N_{C\ IV,i}}{(c/H_0)\sum \Delta X}. \qquad (1)$$

Here, ρ_c represents the (current) critical density, $m_{C\ IV}$ is the mass of the carbon atom, and w_i is the completeness correction applied for each system, as a function of absorber $N_{C\ IV}$ and z (see Figure 2). ΔX represents the comoving absorption pathlength summed over all sightlines, where for each sightline $\Delta X = X(z_{max}) - X(z_{min})$ with

$$X(z) = \frac{2}{3\Omega_M}\sqrt{\Omega_M(1 + z)^3 + \Omega_\Lambda}. \qquad (2)$$
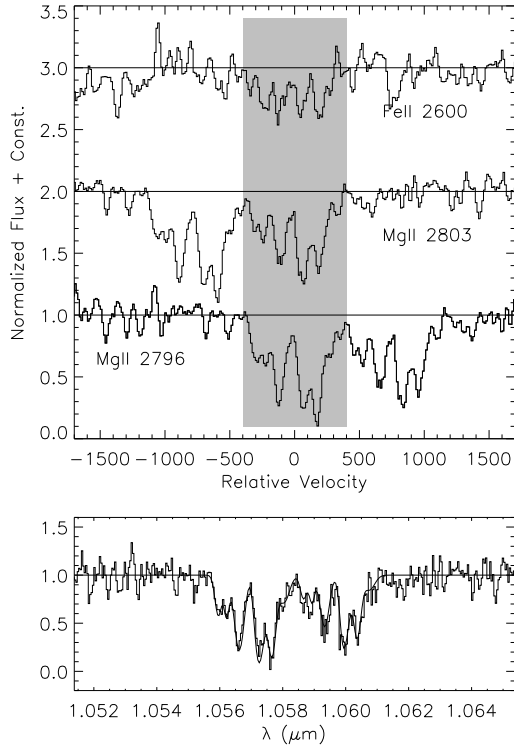
FIG. 5.— Stacked velocity plot showing matched profiles of the Mg II doublet along with Fe II at $z = 2.780$. This identification supersedes prior work which flagged this system as C IV at $z = 5.82$. Note the extremely broad velocity spread, which spans a total of ~ 800 km s^{-1}. At bottom we show a Voigt profile fit to the Mg II complex.

The pathlength for each sightline is listed in Table 1; the integrated path for all FIRE spectra is $\Delta X = 44.93$, of which $\Delta X = 21.92$ is at $z > 5.3$. This is approximately a factor of 4 larger in path than the survey of Becker et al, and 78% larger than the survey of (Ryan-Weber et al. 2009). Many sightlines studied by these authors are in the North and not accessible with FIRE. So, to maximize survey volume we combine separately our FIRE measurements with (primarily NIRSPEC) measurements for northern targets to obtain a total pathlength of $\Delta X = 62.77$, of which $\Delta X = 37.73$ is at $z > 5.3$. Figure 6 shows the resulting calculation of $\Omega_{C\,IV}$, along with independent results at other redshifts, gathered from the literature as listed in the figure caption. We have corrected the point from Ryan-Weber et al. (2009) to remove the Mg II system in SDSS1030+0524.

Several adjustments must be made to put data from different studies together on the same plot, since each survey quotes different levels of completeness, and in some cases different cosmological parameters are used to calculate $\Omega_{C\,IV}$ (Ryan-Weber et al. 2009; Cooksey et al. 2010). For older studies which use an Einstein-deSitter cosmology ($\Omega = 1$) we multiply results by $\sqrt{\Omega_M} \approx 0.55$ to (approximately) translate to currently favored concordance models. A more subtle correction must also be made for weak C IV lines not included in the sum from Equation 1 because of survey incompleteness, which varies from study to study.

This effect may be accounted given knowledge of the column density distribution function $f(N_{C\,IV}) = $

$d\mathcal{N}/dN_{C\,IV}$ for each survey, since $\Omega_{C\,IV}$ may also be expressed as a weighted integral of $f(N)$. The power law slope of f is shallower than $N_{C\,IV}^{-2}$ in all lower redshift surveys, so the effect of missed systems at low $N_{C\,IV}$ is subdominant, but could still represent a factor of ~ 2 or more. We follow the procedures outlined in Ryan-Weber et al. (2009) and Cooksey et al. (2010) to determine the fraction of each survey's systems that would be detected in our sample, appropriately integrating their fits to $f(N_{C\,IV})$ over the range where we are complete. We chose integration limits of $10^{13.4} < N_{C\,IV} < 10^{15}$, since we are sensitive to many systems in this range and our completeness corrections are robust. The fraction of each prior survey's systems that would be detected in the FIRE spectra varies; the specific values we used are 0.70 for Songaila (2001), 0.89 for Songaila (2005), 1.12 for Ryan-Weber et al. (2009), 0.86 for Pettini et al. (2003), and 0.93 for Cooksey et al. (2010). The correction for Ryan-Weber's data relies on the unknown power law slope of $f(N)$ at $z > 5$ which we assumed to run as $N^{-1.5}$; if the slope is as steep as $N^{-1.8}$ then the correction becomes a factor of 1.22.

After all corrections are applied, our principal result is confirmation of a marked decline in $\Omega_{C\,IV}$ at $z > 4.5$, as initially reported by Ryan-Weber et al. (2009) and Becker et al. (2009). We divided up our sample into two redshift bins with $z > 5.3$ and $z < 5.3$, with the lower redshift end extending as low as $z = 4.35$ and the high redshift end to $z = 6.4$. The low redshift bin contains 14 distinct FIRE detections (where we count multi-component systems as single detections), while the high redshift bin contains 5 FIRE detections plus the two likely systems discussed in Section 4.8.1. Our $\Omega_{C\,IV}$ does not include these systems that are not formal detections with FIRE, although the presence of low ionization absorption suggests they are probably real. If we treat our fits to these systems as upper limits to the C IV column density, the amount by which $\Omega_{C\,IV}$ could increase is bounded at 20% (0.08 dex). The total result for the seven FIRE sightlines is $\Omega_{C\,IV} = 6.8 \pm 3.3 \times 10^{-9}$ at $\langle z \rangle = 5.66$, for the column density range $13.4 < \log(N_{C\,IV}) < 15.0$. Similarly the value at $\langle z \rangle = 4.92$ for the FIRE sample alone is $2.0 \pm 0.5 \times 10^{-8}$.

Given the low apparent density of C IV systems, we also re-calculated $\Omega_{C\,IV}$ including 6 sightlines from the literature that were not observed by FIRE. The additional sightlines used include SDSS0002+2550 and SDSS1148+5251, which yielded no detections in high-resolution (23 km s^{-1}) NIRSPEC data (Becker et al. 2009), and SDSS0840+3549, SDSS1137+3549, SDSS1604+4244, and SDSS2054+0054, which were observed at low resolution (185 km s^{-1}) with NIRSPEC by Ryan-Weber et al. (2009). This expanded set of sightlines yields just one additional C IV system, at $z = 5.738$ in SDSS1137+3529. At this system's $\log(N_{C\,IV}) = 14.2$, Ryan-Weber's data should be highly complete so we apply no completeness correction to this system in our modified sum for $\Omega_{C\,IV}$. Becker's spectra, while yielding no detections, should also be highly complete over our full range of column densities given his higher resolution.

The net effect of these largely null results is to reduce the derived density, with our combined value for 13 sight-
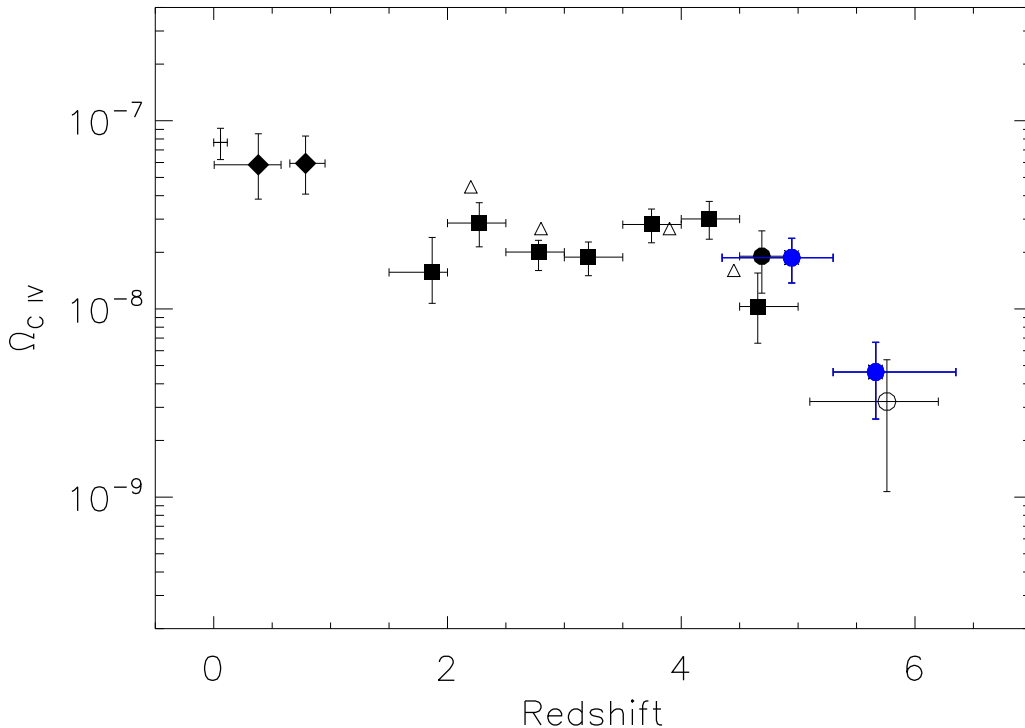
FIG. 6.— Evolution of the mass density in C IV, expressed as $\Omega_{\rm C\ IV}$, for C IV systems with $13.4 \leq \log(N_{\rm C\ IV}) \leq 15.0$. Data from this study are shown in red; the results of several prior studies are shown for comparison, where all are scaled to our fiducial cosmology and corrected for their varying degrees of completeness. Solid squares show results from Songaila (2001), triangles are from Songaila (2005), diamonds are from Cooksey et al. (2010), the cross at $z \approx 0$ is from Danforth & Shull (2008), the solid black circle is from Pettini et al. (2003), and the open black circle is from (Ryan-Weber et al. 2009). Ryan-Weber's point has been adjusted to reflect re-identification of the putative $z = 5.82$ C IV system in SDSS1030 as Mg II.

lines measured at:

$$\Omega_{\rm C\ IV} = \begin{cases} (1.87 \pm 0.50) \times 10^{-8} & \langle z \rangle = 4.95 \\ (0.46 \pm 0.20) \times 10^{-8} & \langle z \rangle = 5.66 \end{cases} \quad (3)$$

The redshifts quoted above reflect the pathlength-weighted mean for each bin, where the lower bin includes all systems from $4.35 < z < 5.3$ and the higher includes all systems with $5.3 < z < 6.4$. While lower than the value from the FIRE spectra alone, the different methods agree to well within 1σ. The values in Equation 3 represent a steady decline in $\Omega_{\rm C\ IV}$ by a factor of 4.1 ± 2.1 over the $4.5 < z < 5.6$ interval. This decline is measured using counts of C IV systems drawn at different redshifts, but from the same spectra.

Our data support the contention that the C IV density is in decline at $z > 4.5$. The exact redshift at which this downturn begins is not strongly constrained by present data, although it appears sometime between $z = 4$ and $z = 5$. When plotted in the context of all surveys including ones in the local universe, several interpretations are possible regarding evolution. Ground based studies to date have focused on the relative constancy of $\Omega_{\rm C\ IV}$ from $2 < z < 5$, followed by a steep drop at higher z. As plotted here, an equally plausible interpretation could be $\Omega_{\rm C\ IV}$ decreasing linearly with increasing redshift from $z = 0$, at constant slope until $z \sim 4.5$ after which the decline quickens. Yet another interpretation

would hold that the C IV mass density is on relatively constant decline over all redshifts, but is enhanced briefly at $z \sim 4$. Coincidentally this is the redshift where the H I cross-section-weighted C IV ionization fraction peaks for a Haardt & Madau (2001) prescription of the ionizing background spectrum. At present the data do not distinguish strongly between these cases; revisiting the $1 < z < 2$ and $z \sim 4$ regions with larger samples of optical spectra should in time be able to settle the question.

6. DISCUSSION

Over the past 5 years, C IV observations at $z > 5$ have evolved from samples of 2 sightlines which were strongly affected by sample variance (Simcoe 2006; Ryan-Weber et al. 2006), to the present sample of 13 sightlines. Yet the number of strong detections has grown slowly, while several sightlines nearly devoid of C IV have now been observed. At a total detection count of 6 sure and 2 likely systems at $z > 5.3$, it is far from clear that we have sampled enough cosmic volume to perform robust statistical analysis.

Yet the data in hand point strongly toward a lower C IV mass density in our high redshift search region. A critical question is to what extent this trend reflects a change in the total carbon abundance as opposed to a change in its ionization balance. Rapid changes such as this over a short timescale are more easily achieved through a combination of radiative and ionization effects rather than chemical feedback, but the period before

$z \sim 3$ was also one of stellar mass buildup in the universe (Bouwens et al. 2007). Some of the byproducts of this process will leak into the IGM, and indeed recent estimates of evolution in the ionization-corrected carbon abundance at $z = 2 - 4$ suggest that the C IV mass in the IGM doubled over this period (Simcoe 2011), although this represents a somewhat longer stretch of time.

The C IV ionization balance is governed principally by photons with energies of 3.5 Ry (C III to C IV), 4.74 Ry (C IV to C V) and > 20 Ry (C V to C VI). These high-energy photons are produced predominantly in AGN, but are also strongly attenuated by intergalactic He II at $z > 4$, since He II reionization likely does not occur until $z \lesssim 3.5$, and perhaps even lower redshift (Shull et al. 2010; Worseck et al. 2011). C IV systems—particularly the strong ones which dominate $\Omega_{\text{C IV}}$—may be preferentially present in He II-ionized bubbles surrounding sites of galaxy formation and/or AGN activity, where the radiation field and abundances are both enhanced.

If the evolution in the C IV abundance is driven by ionization rather than abundance evolution, once might expect to see an increase in the density of low ionization C II, Si II, or O I systems. These systems would arise in regions where abundances are high but the ionizing field is dominated by stellar photons rather than harder AGN radiation.

There are a few lines of evidence hinting at this interpretation for *some* absorbers, though it is still too early to draw definitive conclusions about the general population. Becker et al. (2006) initially reported a strong enhancement in O I absorption toward the high-redshift QSO SDSS1148+5251, and subsequent observations have not yet yielded corresponding C IV absorption coincident with these O I lines. More recent work by Becker et al. (2011) compiles statistics on C II , O I , and Si II absorbers from HIRES and ESI spectra of a large sample of high redshift objects. This study suggests that the evolution of low-ionization absorbers broadly follows the extrapolation of trends established at lower z, with the highly ionized gas phase dropping out at $z \geq 5$. However these studies treat the evolution of low- and high- ionization systems independently, since examples were not available where both ionization phases were detected in a single $z > 5.5$ system.

Two of the systems studied in Becker et al. (2009) are covered by our data on SDSS0818; one of these was first reported as a tentative C IV detection by (Ryan-Weber et al. 2009) and has since also been discussed by D'Odorico et al. (2011). Our data rule out strong C IV absorption in these two systems but admit the possibility of weak lines, while we confirm evidence of low ionization absorption. A small handful of systems are present in our other FIRE spectra with similar low ionization absorption, often identified via Mg II in the H band. Analysis of these systems is outside the scope of this paper, although it is notable that some systems contain strong C IV (and are included in the present sample) and some do not. At the resolution and SNR of our FIRE spectra we do not see evidence for the emergence of a strong "forest" of C II, Si II, or O I lines at $z > 5.5$, although higher quality spectra will be needed to assess this possibility in detail.

Ultimately a combination of abundance and ionization evolution must be at play, suggesting that forward modeling using numerical simulations will be required (Oppenheimer & Davé 2006, 2008; Oppenheimer et al. 2009; Wiersma et al. 2010). If the C IV systems reside in non-overlapping, He II-ionized bubbles, radiative transfer effects and local enrichment are likely to become important. In this case the C IV systems seen at $z > 5.5$ are only "intergalactic" in the sense that they are selected at random from observations of background QSOs. In fact they are likely to be influenced strongly by their environments in both radiation and metal enhancement, and may reside quite close to the early galaxies responsible for reionizing the universe.

7. CONCLUSIONS

Using the newly commissioned FIRE spectrograph, we have observed a sample of seven QSOs at $z > 5.5$ to derive improved constraints on the C IV abundance at early times. Using both manual and automated searches, we identified a sample of 19 lines in our FIRE spectra with C IV column densities in the range $13.2 \leq \log(N_{\text{C IV}}) \leq 14.6$, and redshifts ranging from $z = 4.61$ to 5.91. Monte Carlo tests indicate that our line sample is highly complete at $N_{\text{C IV}} > 10^{14}$ cm^{-2}; it is 50% complete near $10^{13.7}$ cm^{-2} over most survey areas not strongly affected by telluric absorption.

Our conclusions may be summarized as follows:

1. Our spectra show evidence of a decline in the C IV abundance at $z > 5$, consistent with the findings of previous studies not strongly affected by cosmic variance. Expressed in terms of the closure density, we find $\Omega_{\text{C IV}} = 4.6 \pm 2.0 \times 10^{-9}$ at $\langle z \rangle = 5.66$, a four-fold decline relative to what is observed at $\langle z \rangle = 4.95$ and lower redshifts.

2. A strong system in the spectrum of SDSS1030+0524 previously identified in the literature as C IV at $z = 5.82$ is re-identified as Mg II at $z = 2.78$. This system comprised a significant portion of the total C IV mass measured in all prior surveys, so these literature results must accordingly be revised downward.

3. We present new limits on the C IV column density for several systems previously identified based on low-ionization lines and/or weak C IV. The emergence of these systems may reflect an overall change in the ionization balance of absorption systems at $z > 5$, where high-ionization species common at low redshift are less prevalent. Larger statistical samples of these systems could yield interesting model constraints on the evolution of the ionizing background versus metallicity fields

Finally, we caution that as the C IV density drops, even though the number of well-observed sightlines grows our results may still be subject to fluctuations from shot noise or sample variance (only $5 - 7$ systems are now known at $z > 5.5$). The present work summarizes just the first year of an ongoing program to observe high-redshift QSOs. Planned observations should cover the complete catalog of bright, southern-accessible targets, while ongoing and planned surveys such as UKIDSS (Warren et al. 2007), SkyMapper (Keller et al. 2007), and VISTA (McPherson et al. 2006) should substantially

increase the number of known high-z quasars in the Southern sky.

Facilities: Magellan:Baade (FIRE)

It is a pleasure to thank the many engineers and staff at MIT and Magellan who contributed to FIRE's successful construction and commissioning. We gratefully ac-

REFERENCES

Becker, G. D., Rauch, M., & Sargent, W. L. W. 2009, ApJ, 698, 1010
Becker, G. D., Sargent, W. L. W., Rauch, M., & Calverley, A. P. 2011, ArXiv e-prints
Becker, G. D., Sargent, W. L. W., Rauch, M., & Simcoe, R. A. 2006, ApJ, 640, 69
Becker, R. H., et al. 2001, AJ, 122, 2850
Bochanski, J. J., et al. 2009, PASP, 121, 1409
Bond, N. A., Churchill, C. W., Charlton, J. C., & Vogt, S. S. 2001, ApJ, 562, 641
Bouwens, R. J., Illingworth, G. D., Franx, M., & Ford, H. 2007, ApJ, 670, 928
Chen, H., Helsby, J. E., Gauthier, J., Shectman, S. A., Thompson, I. B., & Tinker, J. L. 2010, ApJ, 714, 1521
Cooksey, K. L., Thom, C., Prochaska, J. X., & Chen, H. 2010, ApJ, 708, 868
Cowie, L. L., & Songaila, A. 1998, Nature, 394, 44
Cowie, L. L., Songaila, A., Kim, T., & Hu, E. M. 1995, AJ, 109, 1522
Cushing, M. C., Vacca, W. D., & Rayner, J. T. 2004, PASP, 116, 362
Danforth, C. W., & Shull, J. M. 2008, ApJ, 679, 194
D'Odorico, V., et al. 2011, ArXiv e-prints
Ellison, S. L., Songaila, A., Schaye, J., & Pettini, M. 2000, AJ, 120, 1175
Fan, X., et al. 2006, AJ, 131, 1203
Haardt, F., & Madau, P. 2001, in Clusters of Galaxies and the High Redshift Universe Observed in X-rays
Keller, S. C., Schmidt, B. P., & Bessell, M. S. 2007, ArXiv e-prints
Kelson, D. D. 2003, PASP, 115, 688
Marshall, J. L., et al. 2008, in Society of Photo-Optical Instrumentation Engineers (SPIE) Conference Series, Vol. 7014, Society of Photo-Optical Instrumentation Engineers (SPIE) Conference Series
McPherson, A. M., et al. 2006, in Presented at the Society of Photo-Optical Instrumentation Engineers (SPIE) Conference, Vol. 6267, Society of Photo-Optical Instrumentation Engineers (SPIE) Conference Series

Mortlock, D. J., et al. 2009, A&A, 505, 97
Oppenheimer, B. D., & Davé, R. 2006, MNRAS, 373, 1265
—. 2008, MNRAS, 387, 577
Oppenheimer, B. D., Davé, R., & Finlator, K. 2009, MNRAS, 396, 729
Pettini, M., Madau, P., Bolte, M., Prochaska, J. X., Ellison, S. L., & Fan, X. 2003, ApJ, 594, 695
Prochter, G. E., Prochaska, J. X., & Burles, S. M. 2006, ApJ, 639, 766
Rao, S. M., & Turnshek, D. A. 2000, ApJS, 130, 1
Rauch, M., Sargent, W. L. W., Womble, D. S., & Barlow, T. A. 1996, ApJ, 467, L5+
Ryan-Weber, E. V., Pettini, M., & Madau, P. 2006, MNRAS, 371, L78
Ryan-Weber, E. V., Pettini, M., Madau, P., & Zych, B. J. 2009, MNRAS, 395, 1476
Savage, B. D., & Sembach, K. R. 1991, ApJ, 379, 245
Shull, J. M., France, K., Danforth, C. W., Smith, B., & Tumlinson, J. 2010, ApJ, 722, 1312
Simcoe, R. A. 2006, ApJ, 653, 977
—. 2011, Submitted
Simcoe, R. A., et al. 2010, in Presented at the Society of Photo-Optical Instrumentation Engineers (SPIE) Conference, Vol. 7735, Society of Photo-Optical Instrumentation Engineers (SPIE) Conference Series
Simcoe, R. A., et al. 2011, in
Songaila, A. 2001, ApJ, 561, L153
—. 2005, AJ, 130, 1996
Songaila, A., & Cowie, L. L. 1996, AJ, 112, 335
Vacca, W. D., Cushing, M. C., & Rayner, J. T. 2003, PASP, 115, 389
Warren, S. J., et al. 2007, ArXiv Astrophysics e-prints
Wiersma, R. P. C., Schaye, J., Dalla Vecchia, C., Booth, C. M., Theuns, T., & Aguirre, A. 2010, MNRAS, 409, 132
Willott, C. J., et al. 2010, AJ, 139, 906
Worseck, G., et al. 2011, ArXiv e-prints

TABLE 2
C IV Detections

Object	z_{abs}	$W_r(1548)$[1]	$W_r(1550)$[1]	$N_{\text{C IV}}(AODM$[2]$)$	$N_{\text{C IV}}(VPFIT)$[3]	$b_{\text{C IV}}(VPFIT)$[4]	$\log_{10}(w_i)$[5]
SDSS0818+1722	4.69193	115 ± 23	63 ± 32	13.3 ± 0.20	13.43 ± 0.09	26 ± 13	0.49
$\cdots$	4.72586	462 ± 25	290 ± 17	$> 14.1 \pm 0.03$	13.96 ± 0.04	43 ± 8	0.05
$\cdots$	4.72737	$\cdots$	$\cdots$	$\cdots$	13.67 ± 0.15	10	0.19
$\cdots$	5.78917[6]	37 ± 20	54	$\cdots$	≤ 13.1	$\cdots$	$\cdots$
$\cdots$	5.87689[6]	47 ± 13	33 ± 13	13.3 ± 0.08	≤ 13.41	6.7 ± 8.0	$\cdots$
CFHQS1509-1749	4.61078	26 ± 7	11 ± 8	12.8 ± 0.16	13.23 ± 0.28	5.0 ± 6.0	0.87
$\cdots$	4.64143	71 ± 10	60 ± 10	13.4 ± 0.10	13.44 ± 0.04	48.8 ± 7.0	0.43
$\cdots$	4.66598	89 ± 14	35 ± 11	13.3 ± 0.10	13.41 ± 0.05	40.3 ± 7.7	0.50
$\cdots$	4.81552	308 ± 22	206 ± 19	$> 14.0 \pm 0.10$	14.01 ± 0.04	60.0 ± 5.2	0.06
$\cdots$	4.82492	$\cdots$	33 ± 12	13.2 ± 0.20	13.45 ± 0.09	26.0 ± 10.0	0.63
$\cdots$	5.91578	331 ± 39	183 ± 25	$> 14.1 \pm 0.07$	14.02 ± 0.03	48.8 ± 5.5	0.03
SDSS1030+0524	4.94814	109 ± 27	237 ± 27	13.9 ± 0.07	13.76 ± 0.11	33.8 ± 23.1	0.57
$\cdots$	5.51694	331 ± 31	256 ± 23	$> 14.0 \pm 0.04$	14.02 ± 0.04	72.9 ± 12.0	0.07
$\cdots$	5.72438	698 ± 17	482 ± 18	$> 14.6 \pm 0.03$	14.59 ± 0.04	50.3 ± 3.0	0.04
$\cdots$	5.74399	273 ± 15	172 ± 13	13.87 ± 0.05	14.00 ± 0.04	40.2 ± 5.7	0.05
SDSS0836+0054	4.99623	163 ± 17	73 ± 17	13.6 ± 0.06	13.70 ± 0.05	71.1 ± 11.5	0.63
SDSS1411+1217	5.24988	734 ± 26	321 ± 22	$> 14.3 \pm 0.04$	14.14 ± 0.07	30.0[7]	0.03
$\cdots$	5.24788	$\cdots$	$\cdots$	$\cdots$	13.66 ± 0.10	30.0[7]	0.32
$\cdots$	5.25151	$\cdots$	$\cdots$	$\cdots$	13.95 ± 0.07	30.0[7]	0.11
$\cdots$	5.786[8]	$\cdots$	$\cdots$	$\cdots$	$\cdots$	$\cdots$	$\cdots$
SDSS1306+0356	4.61499	320 ± 13	184 ± 14	13.9 ± 0.03	14.09 ± 0.15	64.4 ± 4.7	0.02
$\cdots$	4.66825	292 ± 31	198 ± 22	$> 14.0 \pm 0.05$	14.07 ± 0.03	58.1 ± 5.8	0.02
$\cdots$	4.86591	1744 ± 50	901 ± 41	$> 14.7 \pm 0.03$	14.80 ± 0.01	80.6 ± 32.3	0.05
$\cdots$	4.87965	514 ± 32	354 ± 30	$> 14.4 \pm 0.10$	14.30 ± 0.20	55.6 ± 19.4	0.06
ULAS1319+0905	5.57415	392 ± 44	196 ± 51	$> 14.1 \pm 0.10$	14.14 ± 0.04	65.5 ± 9.1	0.04
$\cdots$	5.26490	133 ± 33	118 ± 27	13.6 ± 0.15	13.66 ± 0.10	62.9 ± 21.7	0.32

[1] Rest frame equivlent width (mÅ).
[2] Column density (cm^{-2}) determined via the apparent optical depth method (Savage & Sembach 1991). The AODM is formally a lower bound on the column density for saturated doublets, so systems with $N_{\text{C IV}} > 10^{14}$ cm^{-2} are listed as limits in the table.
[3] Voigt profile column density (cm^{-2}).
[4] Voigt profile doppler parameter (km s^{-1}).
[5] Completeness correction (dex)
[6] This system is not a statistically significant C IV system in our spectrum, but we confirm the presence of Si II and other neutral atoms as reported by D'Odorico et al. (2011) and Ryan-Weber et al. (2009). It is *not* included in the $\Omega_{\text{C IV}}$ calculation.
[7] This system is blended such that the uncertainty in b was quite high; this has minimal effect on the total column density.
[8] Intrinsic BAL.